Estimation Theoretic Measure of Resolution for Stochastic Localization Microscopy

James E. Fitzgerald,[1,*] Ju Lu,[2,†] and Mark J. Schnitzer[2,3,‡]

[1]*Department of Physics, Stanford University, Stanford, California 94305, USA*
[2]*Department of Biology, Stanford University, Stanford, California 94305, USA*
[3]*Department of Applied Physics, the CNC Program, and the Howard Hughes Medical Institute, Stanford University, Stanford, California 94305, USA*

(Received 15 November 2011; published 24 July 2012)

One approach to super-resolution fluorescence microscopy, termed stochastic localization microscopy, relies on the nanometer scale spatial localization of individual fluorescent emitters that stochastically label specific features of the specimen. The precision of emitter localization is an important determinant of the resulting image resolution but is insufficient to specify how well the derived images capture the structure of the specimen. We address this deficiency by considering the inference of specimen structure based on the estimated emitter locations. By using estimation theory, we develop a measure of spatial resolution that jointly depends on the density of the emitter labels, the precision of emitter localization, and prior information regarding the spatial frequency content of the labeled object. The Nyquist criterion does not set the scaling of this measure with emitter number. Given prior information and a fixed emitter labeling density, our resolution measure asymptotes to a finite value as the precision of emitter localization improves. By considering the present experimental capabilities, this asymptotic behavior implies that further resolution improvements require increases in labeling density above typical current values. Our treatment also yields algorithms to enhance reliable image features. Overall, our formalism facilitates the rigorous statistical interpretation of the data produced by stochastic localization imaging techniques.

DOI: 10.1103/PhysRevLett.109.048102 PACS numbers: 87.57.cf, 07.05.Pj, 87.57.nf, 87.64.M−

Optical diffraction limits the resolution of conventional fluorescence microscopy, but several super-resolution techniques that circumvent the diffraction limit have recently emerged [1]. Among these, stochastic localization microscopy uses photoswitchable or spontaneous fluorophore transitions between fluorescent and dark states [2–7]. In each imaging cycle, emission from a sparse, random subset of fluorophores enables emitter localization with a precision well beyond the diffraction limit [8,9].

The quantitative relationship between localization precision, labeling density, and image resolution remains unclear. Some groups suppose that the localization statistics of single emitters [9] or emitter pairs [10] set the resolution of stochastic localization microscopy. These are incomplete resolution measures, since they neglect that fine details of the specimen cannot be determined if the labeling is too sparse [2]. Other groups heuristically invoke the Nyquist-Shannon sampling theorem [11] to incorporate labeling density [12]. Here, we argue that this heuristic does not properly describe the role of labeling.

Definitions of resolution exist in both wave optics [13] and estimation theory [10,14]. Here, we consider a feature of the specimen to be resolvable when a microscopist can reliably estimate it from the data. Thus, prior information regarding statistical properties of the object or of the imaging system improves resolution. Single molecule imaging at the nanometer scale depends critically on the prior information that photon emitters are point sources [15]. With extended biological structures, the available prior information about the sample structure typically provides weak constraints. It is unclear to what extent such prior information can suppress spurious labeling details and enhance true object features.

Here, we use estimation theory to find the optimal linear filter for reconstructing a stochastically labeled object using emitter localization data. By comparing the performance of this estimator to the limit that the Cramer-Rao lower bound sets for the variance of any biased estimator, we demonstrate optimality across a broader class of estimators, including those that are nonlinear. Our estimator yields a resolution measure that incorporates the precision of emitter localization, labeling density, and prior information.

We describe the structure of the sample as a spatially varying probability density of fluorescent labels, $s(x)$. Fluorophores are located at $\{x_i\}_{i=1}^{M}$, where the number of emitters is modeled as a Poisson random variable with mean $\bar{M}$. For example, if $\{x_i\}$ are locations of stochastically bound fluorescent antibodies then $s(x)$ is the distribution of antigens, normalized to unity. In stochastic localization microscopy each photon is assigned to a particular emitter, leading to an estimated emitter density function, $d_E(x) = \sum_{i=1}^{M} \delta(x - \hat{x}_i)$. The estimated emitter locations, $\{\hat{x}_i\}$, are distributed about the true locations in a way that depends on the number of detected photons, the pixel size, the background noise, the density of active emitters, and the choice of estimator [4]. In conventional microscopy, the point spread function (PSF), denoted h, describes the

distribution of detected locations of photons emitted by a point source. In stochastic localization microscopy, we use an effective PSF, h_{eff}, to describe the distribution of estimated point source locations for a fixed emitter. Assuming that emitters are equally bright and do not photobleach, the number of photons each fluorophore emits is Poisson distributed with mean $\bar{Q}$. Photobleaching does not strongly affect our results (see the Supplementary Material [16]). When limited by photon counts, $h_{\text{eff}} \approx h^{\bar{Q}}$. Because of the central limit theorem, we model h_{eff} with a Gaussian. Averaging the estimated emitter density function over emitter numbers and locations yields the expected density, $\bar{d}_E = \bar{M}(h_{\text{eff}} * s)$, where * denotes convolution. In comparison, conventional microscopy does not assign photons to emitters, so the recorded data are a photon density with mean $\bar{d}^C = \bar{M}\,\bar{Q}(h * s)$. Here and elsewhere, the superscript C stands for conventional. Thus, stochastic localization microscopy provides images that are sharper than conventional images by approximately the square root of the number of detected photons per emitter.

A frequency-dependent signal to noise ratio (SNR),

$$f(k) \equiv \frac{|\bar{D}_E(k)|^2}{\text{Var}[D_E(k)]} = \bar{M}|H_{\text{eff}}(k)|^2|S(k)|^2, \tag{1}$$

aids intuition for stochastic localization microscopy (see the Supplementary Material [16]). Capital letters denote Fourier transforms of the corresponding functions, and $|S|^2$ is the spectral density of the specimen's spatial structure. The SNR increases linearly with the number of emitters. With sufficiently many emitters, $\bar{M} \gg (|H_{\text{eff}}|^2|S|^2)^{-1}$, the data approach their average values, and one can estimate the underlying structure through deconvolution, $S \approx D_E/(\bar{M}H_{\text{eff}})$. Thus, a linear estimator suffices in the high SNR limit.

Since the effective PSF and the spectral density decline to zero at high spatial frequencies, the SNR also decreases. To analyze stochastic localization microscopy data in this regime, we construct the optimal linear estimator, $\hat{s} \equiv \hat{g} * d_E$, where $\hat{s}$ is the estimated specimen structure and $\hat{g}$ is the filter kernel. Minimizing the average squared error over the ensemble of structures provides the optimal filter in the Fourier domain,

$$\hat{G}_{\langle|S|^2\rangle}(k) = \frac{1}{\bar{M}_{\text{eff}}(k)H_{\text{eff}}(k)(1 + \langle f(k)\rangle^{-1})} \tag{2}$$

(see the Supplementary Material [16]). Here $\langle\cdot\rangle$ denotes the ensemble average, $\bar{M}_{\text{eff}}(k) \equiv \langle\bar{M}|S(k)|^2\rangle/\langle|S(k)|^2\rangle$, and the subscript $\langle|S|^2\rangle$ emphasizes the dependence on the ensemble averaged spectral density. For our theoretical treatment (but not the simulations), we hereon assume for simplicity that the same mean number of emitters label each object in the ensemble, $\bar{M}_{\text{eff}}(k) = \bar{M}$. In the limit of sparse labeling, the kernel approaches $\langle|S|^2\rangle H^*_{\text{eff}}$, attenuating the data. In the opposite limit it approaches the deconvolution filter, $1/(\bar{M}H_{\text{eff}})$. The average SNR mediates the transition between these limits, thereby identifying and enhancing reliable image features.

The expected squared error characterizes the performance of this estimator. The bias and variance of the estimator are $b = -S/(1 + \langle f\rangle)$ and $\text{Var} = (\bar{M}|H_{\text{eff}}|^2(1 + \langle f\rangle^{-1})^2)^{-1}$ (see the Supplementary Material [16]). The squared error, $\epsilon^2 = \text{Var} + |b|^2$, thus satisfies

$$\frac{\epsilon^2[S(k)]}{|S(k)|^2} = \frac{1 + \langle f(k)\rangle\frac{\langle|S(k)|^2\rangle}{|S(k)|^2}}{(1 + \langle f(k)\rangle)^2} \tag{3}$$

(Fig. 1). In the sparse labeling limit, the squared error is entirely bias; in the dense labeling limit, the squared error is all variance. The Fisher information for our model satisfies $(J^{-1})_{k,k} = 1/(\bar{M}|H_{\text{eff}}(k)|^2)$ [14] (see the Supplementary Material [16]), so the Cramer-Rao lower bound implies that the variance of any estimator with our bias function is at least $(\bar{M}|H_{\text{eff}}|^2(1 + \langle f\rangle^{-1})^2)^{-1}$ (see the Supplementary Material [16]). Our estimator achieves this bound.

We use the Cramer-Rao lower bound to compute the minimal squared error of any linearly biased estimator. We find that our estimator captures the optimal linear bias function by minimizing the average squared error with respect to the bias function (see the Supplementary Material [16]). In particular, the optimal linear estimator outperforms all unbiased estimators (Fig. 1), and any superior estimator must be nonlinear and have a nonlinear bias function.

This theoretical performance yields a resolution metric that quantifies the microscopist's ability to estimate the specimen. Above the cutoff frequency,

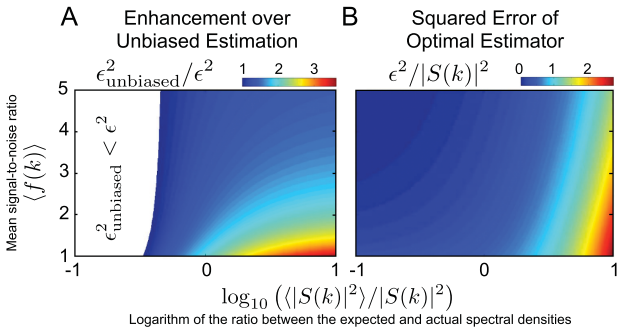

FIG. 1 (color). The optimal linear estimator outperforms any unbiased estimator. (A) We consider how the error associated with the optimal linear estimator compares to the theoretically optimal unbiased estimator ($\epsilon^2_{\text{unbiased}} = 1/(\bar{M}|H_{\text{eff}}(k)|^2)$) as a function of the ratio between the expected and true spectral densities (plotted logarithmically on the x axis) and the mean SNR (y axis). When this ratio is near unity, the optimal linear estimator is superior. At high SNR, the role of the bias decreases, but unbiased estimation is only superior for spatial frequencies present in the specimen but not in the expected spectral density. (B) The expected estimation error as a function of the ratio between the expected and true spectral densities (x axis) and the mean SNR (y axis).

$$k_M \equiv \min\left\{k|\bar{M} \leq \frac{\beta}{|H_{\text{eff}}(k)|^2\langle|S(k)|^2\rangle}\right\}, \quad (4)$$

estimators must suppress signals to avoid noise amplification. The resolution, k_M, is the lowest frequency having SNR below a chosen value of β. At this frequency, a fraction $1/(\beta+1)$ of the deconvolved signal is attenuated. This measure incorporates labeling and prior information and cannot exceed frequencies at which the effective PSF or ensemble spectral density vanish.

To illustrate this point, consider a Gaussian effective PSF, $H_{\text{eff}}(k) = \exp(-\sigma^2 k^2/(2\bar{Q}))$, and a Gaussian ensemble spectral density, $\langle|S(k)|^2\rangle = \exp(-\alpha^2 k^2)$. This spectral density approximates an ensemble of uniform disks (e.g., neurite cross sections) whose radius is proportional to α. Then,

$$k_M = \sqrt{\frac{\bar{Q}}{\sigma^2 + \alpha^2\bar{Q}}\log\frac{\bar{M}}{\beta}} \quad (5)$$

(see the Supplementary Material [16]). For comparison, the optimal filter kernel for conventional microscopy is

$$\hat{G}^{C}_{\langle|S|^2\rangle} = \frac{1}{\bar{Q}\,\bar{M}\,H\left(1 + \frac{1+\bar{Q}|H|^2}{\bar{Q}\,\bar{M}\,|H|^2\langle|S|^2\rangle}\right)}, \quad (6)$$

such that

$$\bar{M} = \beta e^{\alpha^2(k_M^C)^2}(1 + e^{\sigma^2(k_M^C)^2}/\bar{Q}) \quad (7)$$

implicitly defines the cutoff frequency, k_M^C, for the effective PSF and spectral density given above (see the Supplementary Material [16]). Over a broad range of labeling, the cutoff frequency for conventional microscopy varies only modestly, justifying the neglect of labeling density in setting the resolution of conventional microscopy [Fig. 2(a)]. Over the same range, the cutoff frequency for stochastic localization microscopy varies widely, with noticeable resolution changes associated with small changes in labeling [Fig. 2(b)].

We also compare the performance of the optimal linear estimator to other common methods. With some exceptions [17], researchers typically present stochastic localization microscopy data as scattergrams of estimated fluorophore locations [3] or, to emphasize uncertainty, Gaussian profiles at these positions [2]. Direct construction of the optimal filter requires prior knowledge of the ensemble spectral density. We handled the case in which prior knowledge is unavailable by using two iterative methods to approximate the spectral density,

$$S_d^{(0)} = \frac{1}{M}D_E, \qquad G_d^{(i)} = \hat{G}_{|S_d^{(i)}|^2}, \qquad S_d^{(i+1)} = G_d^{(i)}D_E \quad (8)$$

$$S_H^{(0)} = \frac{1}{M}D_E, \qquad G_H^{(i)} = \hat{G}_{|H_{\text{eff}}S_H^{(i)}|^2}, \qquad S_H^{(i+1)} = G_H^{(i)}D_E \quad (9)$$

(see the Supplementary Material [16]). In the limit of infinite SNR, and given the true spectral density, Eq. (8) yields a stable estimate. We prefer Eq. (9) in low SNR situations because it suppresses high-frequency noise. These algorithms may not converge, and we compared the estimates obtained at each of the the first 20 iterations.

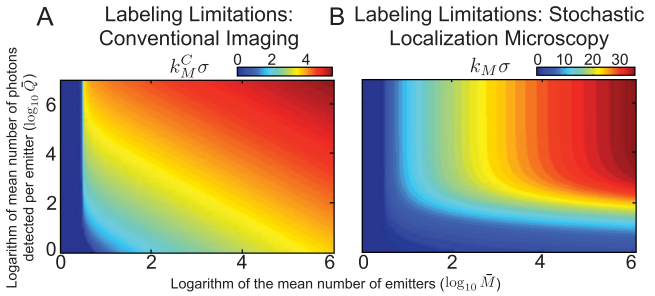

FIG. 2 (color). Labeling density more strongly affects the resolution limit in stochastic localization microscopy than conventional microscopy. We assume that $\alpha^2 = \sigma^2/100$ to approximate an object of radius 15 nm and set $\beta = 3$. Resolution depends both on the average number of emitters that label the object (x axis) and on the average number of photons collected per emitter (y axis). (A) Over the range of relevant labeling densities, the effective resolution in conventional imaging only changes modestly. (B) In stochastic localization microscopy, the achievable resolution varies substantially over the same range of labeling densities. Note the different color scales in (A) and (B).

As an illustration, we considered the problem of reconstructing neuronal axons. Using a set of 256 images of axonal cross sections obtained by confocal microscopy [18], which we assumed would provide a reasonably representative set of axons' shapes, we explored if stochastic localization microscopy would permit reconstruction of axonal shapes at the nanometer scale. We randomly chose 128 images to compute the optimal estimator [Eq. (2)] and used the rest for testing. Figure 3 shows the average performance of several methods over 1000 sessions. The ensemble optimal estimator performed best at all labeling densities, indicating that a library of high resolution structures is likely to facilitate reconstruction via stochastic localization microscopy. Strikingly, with dense labeling both iterative methods that estimate the spectral density outperformed methods that ignore the spectral density, but with sparse labeling these methods performed poorly. A single iteration of one of these algorithms is usually sufficient to obtain its lowest error.

In summary, we have defined an estimation theoretic measure of resolution for stochastic localization microscopy that incorporates localization precision, labeling density, and specimen statistics. One can potentially use a library of electron microscopy images to obtain the prior information needed to attain this resolution limit. This idea is appealing in neuroscience, in which efforts to reconstruct neural circuitry are striving for immense data sets [19]. When such data are unavailable, researchers may use Eqs. (8) or (9) to approximate the filter.

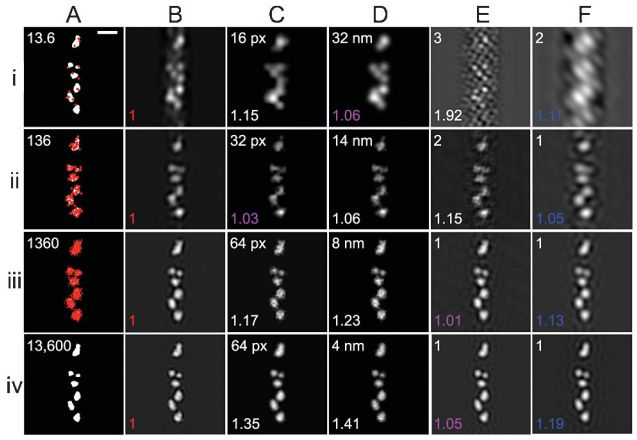

FIG. 3 (color). Optimally filtered data approximate axonal cross sections more accurately than standard methods. We thresholded and rescaled each image in the data set [18] to have 2 nm × 2 nm pixels and simulated stochastic localization microscopy with a Gaussian effective PSF whose standard deviation is 14 nm. Rows show different peak labeling densities: (i) 500 μm^{-2}, (ii) 5×10^3 μm^{-2}, (iii) 5×10^4 μm^{-2}, (iv) 5×10^5 μm^{-2}. Columns show different reconstruction methods: (A) true specimen structure (200 nm scale bar) with estimated emitter locations shown for (Ai)-(Aiii); (B) estimate from the optimal linear filter; (C) estimate formed by reducing the number of pixels, which smooths the image; (D) estimate from Gaussian smoothing; (E) estimate from Eq. (8); (F) estimate from Eq. (9). Numbers in the lower left specify the average error over 1000 sessions. We report errors in multiples of the error from the optimal linear filter at the same labeling density. Numbers in the upper left represent method parameters: (A) mean number of emitters that label the displayed image; (C) number of pixels per side; (D) standard deviation of the Gaussian kernel; (E)–(F) number of iterations. All method parameters were optimized for each labeling density to minimize the method's error. For each labeling density, we write the smallest error in red, the second smallest in violet, and the third smallest in blue. We chose the displayed axonal specimen randomly.

Our estimator is optimal within a broad class, but strongly biased nonlinear methods may surpass our resolution limit. Our estimator and limit depend only on the first two moments of the estimated emitter density function. Since the noise is not Gaussian, higher moments may contain additional information that researchers can use to design more sophisticated estimators.

Our resolution measure generally attains a finite value, even with infinite photon counts (see the Supplementary Material [16]). A few hundred photons per emitter can be sufficient [Fig. 2(b)]. This localization precision is experimentally achievable [20]. Improving the resolution by increasing the labeling density of antibody-conjugated fluorophores [3,5] is nontrivial because of their substantial size relative to the features one wants to resolve. Fluorescent proteins and synthetic dye molecules are generally smaller [21], so use of these may facilitate denser labeling.

Although denser labeling improves resolution, the Nyquist criterion suggests an overly optimistic scaling, $k_M^{\mathrm{Nyq}} \sim \sqrt{M}$. In our treatment, the resolution generally scales as $\sqrt{\log M}$ (see the Supplementary Material [16]). This dependence reflects a balance between the linear increase of SNR with labeling density and the Gaussian decrease with frequency. Fundamentally, the Nyquist sampling theorem does not set the scaling because observing a single emitter's position is not equivalent to sampling an image intensity.

In comparison to traditional notions of resolution, the achievable resolution depends on the specimen. A specimen with spectral density concentrated at low frequencies will constrain the resolution limit because it lacks signal (SNR) at high frequencies. This does not preclude satisfactory image reconstruction, because high frequencies are irrelevant in this context. Given a fixed ensemble of specimens, our theory clarifies the labeling density and localization precision needed to estimate a specimen's spatial frequency components.

The authors thank Eran Mukamel and Brian Wilt for helpful comments. J. E. F. acknowledges support from the National Science Foundation and an NSF IGERT traineeship under 0801700. M. J. S. acknowledges support from the W. M. Keck Foundation and NIH Director's Pioneer (DP1OD003560). J. E. F. and J. L. contributed equally to this work.

*jamesef@stanford.edu
†julu@stanford.edu
‡mschnitz@stanford.edu

[1] B. A. Wilt, L. D. Burns, E. T. W. Ho, K. K. Ghosh, E. A. Mukamel, and M. J. Schnitzer, Annu. Rev. Neurosci. **32**, 435 (2009).
[2] E. Betzig, G. H. Patterson, R. Sougrat, O. W. Lindwasser, S. Olenych, J. S. Bonifacino, M. W. Davidson, J. Lippincott-Schwartz, and H. F. Hess, Science **313**, 1642 (2006).
[3] M. J. Rust, M. Bates, and X. Zhuang, Nat. Methods **3**, 793 (2006).
[4] S. T. Hess, T. P. K. Girirajan, and M. D. Mason, Biophys. J. **91**, 4258 (2006).
[5] M. Bates, B. Huang, G. T. Dempsey, and X. Zhuang, Science **317**, 1749 (2007).
[6] M. Heilemann, S. van de Linde, M. Schuttpelz, R. Kasper, B. Seefeldt, A. Mukherjee, P. Tinnefeld, and M. Sauer, Angew. Chem. Int. Edit **47**, 6172 (2008).
[7] J. Foelling, M. Bossi, H. Bock, R. Medda, C. A. Wurm, B. Hein, S. Jakobs, C. Eggeling, and S. W. Hell, Nat. Methods **5**, 943 (2008).
[8] C. S. Smith, N. Joseph, B. Rieger, and K. A. Lidke, Nat. Methods **7**, 373 (2010).
[9] K. I. Mortensen, L. S. Churchman, J. A. Spudich, and H. Flyvbjerg, Nat. Methods **7**, 377 (2010).
[10] S. Ram, E. Ward, and R. Ober, Proc. Natl. Acad. Sci. U.S.A. **103**, 4457 (2006).
[11] C. Shannon, Proc. IRE **37**, 10 (1949).

[12] H. Shroff, C. G. Galbraith, J. A. Galbraith, and E. Betzig, Nat. Methods **5**, 417 (2008).
[13] J. W. Goodman, *Introduction to Fourier Optics* (McGraw-Hill Science/Engineering/Math, New York, 1996).
[14] E. A. Mukamel and M. J. Schnitzer, Phys. Rev. Lett. (to be published).
[15] A. Yildiz, J. Forkey, S. McKinney, T. Ha, Y. Goldman, and P. Selvin, Science **300**, 2061 (2003).
[16] See Supplemental Material at http://link.aps.org/supplemental/10.1103/PhysRevLett.109.048102 for mathematical derivations and further discussion of key results.
[17] D. Baddeley, M. B. Cannell, and C. Soeller, Microsc. Microanal. **16**, 64 (2010).
[18] J. Lu, J. C. Tapia, O. L. White, and J. W. Lichtman, PLoS Biol. **7**, 265 (2009).
[19] Y. Mishchenko, T. Hu, J. Spacek, J. Mendenhall, K. M. Harris, and D. B. Chklovskii, Neuron **67**, 1009 (2010).
[20] B. Huang, W. Wang, M. Bates, and X. Zhuang, Science **319**, 810 (2008).
[21] X. Michalet, F. Pinaud, L. Bentolila, J. Tsay, S. Doose, J. Li, G. Sundaresan, A. Wu, S. Gambhir, and S. Weiss, Science **307**, 538 (2005).